https://doi.org/10.5194/egusphere-2026-4212
Preprint. Discussion started: 28 August 2026

High-resolution ensemble projections of ocean warming and sector-specific indices in the North and Baltic Seas

Birte-Marie Ehlers[1], Jian Su[2], Frank Janssen[1], and Kristine Skovgaard Madsen[2]

[1]Federal Maritime and Hydrographic Agency, Operational Modeling, Neptunallee 5, 18057, Rostock, Germany
[2]Danish Meteorological Institute, Weather Research, Sankt Kjelds Plads 11, 2100, Copenhagen, Denmark

Correspondence: Birte-Marie Ehlers (Birte-Marie.Ehlers@bsh.de)

Abstract. This study investigates future temperature changes in the surface and benthic layers of the North Sea and the Baltic Sea using a high-resolution, three-dimensional regional hydrodynamic ensemble. To simulate future ocean states, we forced our regional ocean model with a five-member atmospheric ensemble from EURO-CORDEX, using their dynamically downscaled variables under the high-emission RCP8.5 pathway across three 30-year climatological time slices: historical (1971–2000), near-future (2031–2060), and far-future (2071–2100). Rigorous validation against long-term satellite observations reveals systematic, seasonally dependent model biases, marked by winter overestimation and summer underestimation of sea surface temperatures (SST). To mitigate these anomalies, a monthly linear scaling (MLS) bias correction scheme is implemented. Projections indicate an accelerated three-dimensional warming trend toward the end of the century, with pronounced regional hotspots exceeding 4–5 °C in semi-enclosed arctic-amplification zones like the Bothnian Bay and the Gulf of Finland. To demonstrate why bias correction is vital and to illustrate the socioeconomic and ecological value of bias-corrected projections, the model results are converted into two sector-specific indicators. The surface-based "bathing suitability index" reveals an expansion of water temperatures above 20 °C along the western Baltic coast, indicating prolonged tourist seasons alongside heightened risks of pathogenic *Vibrio* proliferation. Moreover, the bottom-based "spawning survival index" suggests that spring sea bottom temperatures (SBT) in the North Sea will consistently transcend the optimal 7 °C threshold for Atlantic cod (*Gadus morhua*), driving an inevitable northward habitat migration. These results highlight the critical necessity of surface and vertical bias correction when deploying hydrodynamic models to inform regional climate adaptation frameworks.

1 Introduction

The global ocean acts as the primary thermal regulator of the Earth's climate system (Levitus et al., 2000). Over the past six decades, both observational networks and climate simulations have documented a profound marine warming trend driven by increased net surface heat fluxes of anthropogenic origin (Pierce et al., 2006; Tyrrell, 2011; IPCC, 2021). Rather than being a passive sink, the ocean dynamically responds to this accumulated heat, altering moisture and energy exchanges with the atmosphere, which subsequently shifts regional weather regimes and amplifies extreme meteorological events (Rahmstorf and Coumou, 2011; Diffenbaugh et al., 2017; Dangendorf et al., 2021). While the deep open ocean exhibits a delayed response to global thermal forcing, shallow and semi-enclosed marginal seas represent critical early-response frontlines for climate change

https://doi.org/10.5194/egusphere-2026-4212
Preprint. Discussion started: 28 August 2026

impacts (Diffenbaugh et al., 2017; Wang and Wu, 2022). Known as 'constrained geometries' and 'intimate coupling with localised atmospheric conditions', these systems possess small thermal capacities that cause them to respond more rapidly and intensely to ambient warming than the global ocean average (Schroeder et al., 2017; Cheng et al., 2022). Among Europe's marginal waters, the North Sea and the Baltic Sea represent socio-economically and ecologically vital environments that are uniquely vulnerable to these accelerated climatic shifts (Backhaus, 1996; Meier et al., 2004; Ducrotoy and Elliott, 2008; Meier et al., 2022; Reckermann et al., 2022).

Characterised by shallow bathymetry and intricate hydrodynamics, the North and Baltic Seas serve as critical sentinel regions for monitoring climate change impacts (Dieterich et al., 2019). Thermally induced stress is already forcing a structural transformation of local marine ecosystems (Dulvy et al., 2008; Engelhard et al., 2014). This ecological shift in the North Sea is most clearly manifested in poleward shifts of species distributions; traditional cold-water commercial stocks, such as Atlantic cod (*Gadus morhua*), are retreating northward into deeper, cooler zones (Engelhard et al., 2014; Huserbråten et al., 2018; Gordó-Vilaseca et al., 2024), while temperate-water species like sea bass and anchovy increasingly inhabit the warming niches (Townhill et al., 2023). In the brackish Baltic Sea, surface warming further exacerbates water column stratification. This process restricts vertical mixing, intensifies seasonal hypoxia in deep basins, and expands macro-benthic "dead zones" (Conley et al., 2009, 2011; Carstensen and Conley, 2019). These ecosystem-level adjustments carry severe economic consequences for regional commercial fisheries, forcing them to rapidly adapt to volatile stock configurations (Van Der Meeren and Ivannikov, 2006). Concurrently, coastal economies face a contradictory reality: while escalating sea surface temperatures (SST) may extend the profitable summer tourism season, this warming directly accelerates public health hazards, including toxic harmful algal blooms (HABs) and the virulent proliferation of pathogenic bacteria such as *Vibrio* spp. in recreational waters (Krupska et al., 2024).

Developing robust regional adaptation and mitigation frameworks requires highly detailed and physically reliable climate projections for local decision-makers (Madsen et al., 2019). Although Global Climate Models (GCMs) establish the foundational baseline for future greenhouse gas trajectories, their coarse structural resolution cannot resolve the intricate coastlines, shallow bathymetry, and complex hydrodynamics characteristic of European marginal seas (Meier, 2006; Pierce et al., 2009; Feser et al., 2011; Meier et al., 2012). Consequently, many historical regional assessments have been restricted to the sea surface, leaving critical data gaps regarding Sea Bottom Temperature (SBT) variations that dictate the health of benthic ecosystems and demersal fish stocks (Meier et al., 2018). Furthermore, even state-of-the-art, high-resolution regional ocean models remain prone to systematic errors inherited from atmospheric drivers (Christensen et al., 2022). In our target domains, uncorrected simulations frequently exhibit pronounced, seasonally dependent biases, characterised by a distinct overestimation of winter temperatures and an underestimation of summer peaks. If left uncorrected, these biases can lead to heavily distorted threshold-dependent assessments, drastically underreporting the projected frequency of marine heatwaves or pathogenic outbreaks (Teutschbein and Seibert, 2012). There is a clear need for robust, three-dimensional modeling efforts that can translate raw physical variables into bias-corrected, sector-specific indices for policy and planning applications.

To address these critical research gaps, this study presents a high-resolution, three-dimensional ensemble projection tracking both surface and sea bottom warming across the North and Baltic Seas through the 21st century. Utilising the baroclinic

https://doi.org/10.5194/egusphere-2026-4212
Preprint. Discussion started: 28 August 2026

HIROMB-BOOS Model (HBM) nested framework, we downscale a five-member atmospheric ensemble from the EURO-CORDEX project under the high-emission RCP8.5 scenario (Jacob et al., 2014, 2020) for the mid- (2031–2060) and late-century (2071–2100) windows. A focal point of this work is the development and application of a monthly linear scaling (MLS) bias correction scheme across the vertical water column to optimise model reliability against observational satellite benchmarks. Finally, we translate this refined physical data into applied management metrics—specifically targeting a "bathing suitability index" for coastal tourism and a "spring survival index" for commercial cod spawning—delivering actionable, localised climate intelligence to anchor regional adaptation strategies.

2 Data and climate simulations

2.1 Observational data for validation and bias correction

A high-resolution, satellite-derived SST dataset was used as the observational benchmark for validating a model hindcast simulation, evaluating the model's historical simulations, and performing the subsequent bias correction of the ensemble projections. This reference dataset is a long-term Climate Data Record (CDR) specifically developed for the North Sea and Baltic Sea, as detailed in Høyer and Karagali (2016). The data were provided by the Danish Meteorological Institute (DMI) and the Copernicus Marine Environment Monitoring Service (CMEMS, 2026a). For validating the hindcast simulation, observational data from 1982–2018 were utilized. For calculating the monthly bias, the daily observational data were averaged over the reference period of 1982–2005 to establish a stable climatology against which the model's performance was assessed.

For the validation of the water column temperature data, Atlantic-European North West Shelf-Ocean In-Situ Near Real Time observations from CMEMS (CMEMS, 2026b) were used as mean profiles. The temporal availability of data varies by station, and continuous, large-scale sea bottom temperature observations are not available for the study region.

2.2 Climate simulations setup

To assess future changes in ocean temperature, numerical simulations were conducted for three distinct 30-year time slices following the methodology established by Cubasch et al. (1995): a historical reference period (1971–2000), a near-future period (2031–2060), and a far-future period (2071–2100). Future projections were carried out under the high-emissions Representative Concentration Pathway 8.5 (RCP8.5) scenario, providing an assessment of high-end regional climate risk.

The ocean simulations were executed using the HIROMB-Boos Model (HBM), which is a three-dimensional, baroclinic regional ocean model (Berg and Poulsen, 2012; Andrée et al., 2021, 2022). The model setup (Fig. 1) covers the North Sea and the Baltic Sea with an interactive two-way nesting system (Su, 2022). The parent domain features a horizontal resolution of approximately 5.5 km with 50 vertical layers. It dynamically nests two higher-resolution sub-domains: the German Bight at ∼1.8 km resolution (24 layers) and a region covering the Kattegat, Danish Straits, and Western Baltic Sea at ∼0.9 km resolution (52 layers). This version of HBM (v2.8) stems from an extensively validated operational storm surge prediction framework (Berg and Poulsen, 2012; Fu et al., 2012; She and Nielsen, 2019; Su et al., 2022; Andrée et al., 2023; Su et al., 2024). To

https://doi.org/10.5194/egusphere-2026-4212
Preprint. Discussion started: 28 August 2026

ensure structural robustness, a continuous historical hindcast (1961–2018) was completed using high-resolution atmospheric fields from the UERRA (Uncertainties in Ensembles of Regional Re-Analyses) HARMONIE/V1 regional reanalysis dataset for Europe (Ridal et al., 2017).

Crucial to the high-resolution multi-decadal simulation setup is the handling of the open lateral boundaries connecting the North Sea to the open Atlantic Ocean. Prescribing temperature and salinity boundary conditions in a regional climate downscaling context introduces structural trade-offs. Rather than utilising fully dynamic variables extracted directly from raw global climate models (GCMs), we applied a multi-decadal linear trend option at the open boundaries following the methodology established by Tian et al. (2016). Dynamic boundary conditions are omitted here because the decadal-scale intrinsic variability inherent in GCMs remains highly unreliable for specific future decades and is outside the scope of this long-term centennial warming assessment. By isolating the external thermodynamic boundary forcing to a linear trend, we insulate the marginal basins from unrepresentative GCM-derived decadal oscillations while preserving structural mass and heat transport signals entering the North Sea (Tian et al., 2016).

For the climate projection runs, the ocean model was driven by daily atmospheric variables extracted from five independent regional climate model configurations from the EURO-CORDEX project (Table 1) (Jacob et al., 2014, 2020). This regional atmospheric ensemble relies on dynamically downscaled products originating from the Coupled Model Intercomparison Project Phase 5 (CMIP5) core generation. The selection of CMIP5-downscaled inputs over newer CMIP6 equivalents is dictated by data availability; at present, dynamically downscaled CORDEX products driven by CMIP6 global lines do not possess a sufficiently large multi-model ensemble matrix over northern Europe to support a reliable regional uncertainty analysis. Additionally, this configuration remains highly representative, as the historical RCP8.5 scenario and the newer Shared Socioeconomic Pathway equivalent (SSP5-8.5) follow nearly identical atmospheric and radiative forcing trajectories through the end of the twenty-first century.

The selection of the five specific atmospheric configurations from the broader EURO-CORDEX matrix was guided by two primary scientific criteria. First, we prioritised the availability of sub-daily atmospheric forcing fields. Access to sub-daily variables is a strict prerequisite for high-resolution regional ocean modelling, as coarse daily averaged atmospheric inputs artificially smooth out turbulent energy transfers. High-frequency forcing is essential for accurately simulating extreme marine events, such as marine heatwaves. Second, the ensemble exclusively compiles RCMs developed and maintained by specialised meteorological institutions located within Northern Europe (Table 1). This geographical constraint ensures domain-specific parameter optimisation. The physical parameterisation schemes within these localised RCMs—particularly regarding planetary boundary layer structures, sub-grid scale maritime cloud dynamics, and high-latitude air-sea-ice thermodynamic interactions—have been rigorously tuned and calibrated for the specific climatic regimes of the North Sea and the Baltic Sea. Utilising models optimised for these epicontinental basins drastically reduces systemic boundary layer distortions compared to generalised pan-European setups, maximising the physical reliability of the downscaled hydrodynamic fields.

Consequently, the compiled EURO-CORDEX multi-model ensemble presents a physically robust and rigorous configuration to sample regional projection uncertainty arising from different atmospheric structures, extreme wind speed projections, and atmospheric energy transfers under a high-forcing scenario.

https://doi.org/10.5194/egusphere-2026-4212
Preprint. Discussion started: 28 August 2026

2.3 Bias correction: monthly linear scaling

Validating the historical model runs against observational data revealed systematic, seasonally locked discrepancies. The model ensemble universally exhibited an overestimation of temperature in winter and an underestimation during the summer peak. To prevent these systematic errors from confounding absolute thresholds in downstream socio-ecological applications, a MLS bias correction scheme was applied to the sea surface and bottom temperature layers at each model grid cell across all five ensemble members. This method isolates and corrects the mean error for each calendar month independently, thereby preserving the underlying daily variability, non-linear trends, and long-term climate change signals generated by the model.

The correction was implemented in two successive steps for each calendar month ($m = 1, \ldots, 12$):

1. **Calculating the monthly bias:** For each month m, the long-term bias (B_m) was defined as the difference between the multi-year monthly mean of the historical model run ($\overline{M_{\mathrm{hist,m}}}$) and the corresponding monthly mean of satellite observations ($\overline{O_{\mathrm{hist,m}}}$) over the common reference period 1982–2005:

$$B_m = \overline{M_{\mathrm{hist,m}}} - \overline{O_{\mathrm{hist,m}}} \tag{1}$$

   To avoid artificial temperature steps at monthly boundaries in daily resolved time series, the calculated multi-year monthly values are continuously interpolated across daily timesteps, guaranteeing a smooth transition at the turn of the month.

2. **Applying the correction:** The calculated monthly bias B_m was then subtracted from the daily raw future simulation time series ($M_{\mathrm{raw,fut}}$) for the matching month to yield the corrected projection series ($M_{\mathrm{corr,fut}}$) for both future slices:

$$M_{\mathrm{corr,fut}}(t) = M_{\mathrm{raw,fut}}(t) - B_m, \quad \text{for any time } t \text{ in month } m \tag{2}$$

This protocol was performed individually for each of the five ensemble members to address their specific atmospheric forcing biases. Because large-scale, deep-water calibration arrays are sparse, the applicability of surface-derived MLS to bottom layers was cross-evaluated. For the validation of sub-surface layers, quality-controlled vertical ocean profiles from the EN4 dataset (Good et al., 2013) were utilized. Exclusively in sectors characterized by tight vertical coupling and comprehensive seasonal mixing, the surface-derived correction was extended to the sea bottom layer.

2.4 Model ensemble generation

Following bias correction, the five calibrated members (M) were integrated into unified historical and future ensemble mean matrices (E) to represent the central tendency of the projections:

$$E_{\mathrm{hist}} = \frac{1}{n}\sum_{i=1}^{5} M_{\mathrm{hist,i}} \tag{3}$$

$$E_{\mathrm{fut}} = \frac{1}{n}\sum_{i=1}^{5} M_{\mathrm{fut,i}} \tag{4}$$

https://doi.org/10.5194/egusphere-2026-4212
Preprint. Discussion started: 28 August 2026

3 Results

3.1 Model validation and impact of bias correction

3.1.1 Sea surface temperature

The reanalysis-driven hindcast run (1961–2018) was validated against satellite SST records for the period 1982–2018 (Fig. 3). On an annual basis, the model shows a minimal net bias of 0.12 °C. However, distinct seasonal signals emerge upon partitioning: a cold bias averaging −0.23 °C occurs during winter (DJF), whereas a warm bias averaging 0.44 °C dominates during summer (JJA), with peak errors clustering within shallow coastal zones.

When driven by the EURO-CORDEX climate forcing during the historical period (1982–2005), the uncorrected ensemble members manifest diverse, structurally significant seasonal errors (Fig. 4). In winter, the ensemble members exhibit diverging bias signs; the REMO2009 setup displays a strong warm bias up to 1–2 °C across the North Sea, while the KNMI model generates a cool bias of equivalent magnitude. All models show a warm bias for large parts of the Baltic Sea. Only Baltic shallow coastal areas and the Danish Straits in the KNMI model show a cold bias. In contrast, a systematic model bias emerges during summer: four out of five members underestimate SST by more than -2 ° across the shallow coastal plains of the German Bight, the southern North Sea and the Baltic Sea.

The impact of applying the MLS correction is shown for the Lightship German Bight station (Figs. 5 and 2). Prior to correction, the raw ensemble mean deviates from the annual curve, overestimating winter-to-spring transitions and underestimating summer peaks. Following the application of MLS, the calibrated ensemble mean achieves near-perfect alignment with the observational climatology (Fig. 5b), successfully removing systematic distortion before projecting absolute threshold indices.

3.1.2 Temperature in the water column

To evaluate whether surface-derived bias corrections can improve three-dimensional water column profiles, uncorrected and corrected configurations were compared against sparsely available CMEMS in-situ vertical profile observations from 1990–2005 at key stations in the German Bight and the western Baltic Sea. Raw configurations exhibit severe vertical scatter. Once corrected, the observed in-situ data profiles settle within the first standard deviation of the ensemble mean at the differnet stations. Crucially, the temperature bias remains vertical and isotropic, meaning the offset resolved at the surface maintains structural consistency down through the deep layers. This indicates that surface-derived adjustments can successfully calibrate water column profiles in well-mixed areas.

3.1.3 Sea bottom temperature

To evaluate the physical validity of extending surface corrections to benthic layers, a cross-correlation and time-lag analysis was executed for the North Sea for March and April (Figs. 6). Across the shallow reaches of the German Bight, SST and SBT demonstrate a high correlation coupled with a zero-day temporal lag, indicating instantaneous vertical convective mixing.

https://doi.org/10.5194/egusphere-2026-4212
Preprint. Discussion started: 28 August 2026

Seasonal assessments of benthic temperature across the German Bight showcase distinct thermal shifting patterns (Fig. 7). The absolute difference map between the uncorrected and corrected benthic layers isolates two structural zones: uncorrected coastal waters are up to 2.0 ° too cold in winter and 3.3 °C too cold in spring, whereas offshore benthic layers are artificially warm.

3.1.4 Ensemble historical and projection envelopes

Daily resolved SST curves tracking the historical reference, near-future, and far-future envelopes for the Lightship German Bight station elucidate the damping effects of bias correction on variance (Fig. 8). While the daily historical variability of individual projections is preserved, the inter-model spread within the 5th and 95th percentiles narrows.

As compiled in Table 2, the baseline shifts dramatically under the RCP8.5 scenario. At Lightship German Bight, the uncorrected historical summer maximum rises from 18.1 °C to 21.0 °C by 2100. Once corrected via MLS, the physical baseline adjusts upward, revealing that true late-century peak summer exposures will reach an absolute ensemble mean of 21.8 °C.

3.2 Projected spatial warming trends and hotspots

Analysis of regional monthly means and corresponding anomalies reveals an overarching warming trend across the North Sea and the Baltic Sea (Fig. 9). The multi-model framework projects an absolute mean basin-wide warming of 1.5–2 °C for the near-future period, expanding to ∼3 °C by the far-future horizon, with warming rates accelerating over time.

Spatial heterogeneity is highly pronounced, with the land-locked Baltic Sea warming more intensely than the open North Sea (Tables 3 and 4). The most severe warming hotspots are projected within sub-arctic marginal boundaries. During May and June in the late-century window, warming anomalies exceed 5 °C in the Bothnian Bay and 4 °C in the Gulf of Finland, demonstrating a localized amplification process.

3.3 Regional projections and sector-specific indices

3.3.1 Index for bathing temperature: Exceeding summer temperature of 20°C

The surface indicator for bathing suitability was evaluated across the shallow coastal waters of the western Baltic Sea (Figs. 2 and 10). During the historical reference timeframe (1971–2000), the 20 °C suitability and safety threshold was never exceeded (Table 5). Under the RCP8.5 scenario, threshold-transgressing events change from rare anomalies in the near future to regular annual phenomena by the late century.

The application of bias correction substantially alters the calculated duration of these events. Taking the simulation year 2086 as a representative example (Fig. 10b), the corrected time series predicts a much longer and more intense period above the threshold compared to the raw data. Across the far-future slice, the total cumulative count of threshold-exceeding days increases by a factor of five between uncorrected (344 days) and corrected (1329 days) configurations, yielding an average annual difference of 34 days (Table 5).

https://doi.org/10.5194/egusphere-2026-4212
Preprint. Discussion started: 28 August 2026

3.3.2 Index for spawning of Atlantic cod: Exceeding spring temperature (7°C and 9.6°C)

The benthic indicator tracking commercial spawning constraints for Atlantic cod (*Gadus morhua*) was calculated across the North Sea during March and April (Fig. 11 and Table 6). The index maps daily exceedance against two biophysical limits: the optimal preferred spawning boundary (7 °C) and the maximum tolerable survival ceiling (9.6 °C). In the historical baseline, conditions exceeding 7 °C occurred only during isolated anomalies (78 corrected days across 30 years), and the 9.6 °C ceiling was never breached.

In the near-future horizon, the corrected ensemble mean shows that bottom water temperatures will routinely exceed the optimal 7 °C limit, spending a cumulative 1284 days above it. By the late-century window, the North Sea benthic layer warms so excessively that the 7 °C optimal threshold is breached continuously throughout March and April (1830 total days). Furthermore, the critical 9.6 °C survival ceiling begins to fail regularly toward late April. The calculation of these failure rates is highly sensitive to the bias correction method; the corrected configuration yields 35 days of total reproductive ceiling failure, compared to only 6 days predicted by raw model output.

4 Discussion

4.1 Implications of bias correction on risk assessment

This investigation demonstrates that raw regional hydrodynamic models exhibit systematic seasonal temperature errors that can compromise their utility for direct impact assessments. If left uncorrected, the summer cold bias inherent across most EURO-CORDEX-driven HBM members leads to an underestimation of absolute extreme temperatures. Such an underestimation could misinform regional adaptation strategies, particularly regarding threshold-dependent biological and public health hazards.

For example, our surface metric highlights that uncorrected results would cause planners to underestimate the duration of warm-water days (> 20 °C) along western Baltic resort tracts by approximately one month per year. This has real-world implications, as water temperatures exceeding 20 °C act as primary triggers for the exponential growth of pathogenic *Vibrio* bacteria and harmful algal blooms (HABs). Consequently, using uncorrected physical data would result in an underestimation of environmental health risks.

A similar issue appears when evaluating benthic ecosystems. While continuous data collection at the sea bottom remains limited, both our validation against vertical profiles and a cross-correlation analysis confirms that applying an MLS correction to deeper water layers is a scientifically sound approach for well-mixed, shallow shelf seas. In terms of fisheries management, using uncorrected simulations would lead to an underestimation of the thermal stress experienced by demersal stocks. The corrected model shows a much higher frequency of late-century failures for the cod spawning ceiling (9.6 °C) than raw model projections, highlighting the importance of bias correction for accurate risk assessment.

The necessity of addressing these distortions has traditionally led researchers to employ the delta change method, wherein simulated future climate anomalies (the "deltas") are added to historical baseline observations (Navarro-Racines et al., 2020). While this approach circumvents raw model biases by anchoring projections to a realistic historical baseline, it suffers from

https://doi.org/10.5194/egusphere-2026-4212
Preprint. Discussion started: 28 August 2026

several critical limitations (Teutschbein and Seibert, 2012). Crucially, the delta change method assumes that baseline climate variance and seasonal cycles remain stationary, thereby failing to capture non-linear modifications in climate variability, shifting seasonal envelopes, or intensified extreme events. Furthermore, the method is fundamentally restricted by the scarcity of high-quality historical observations, particularly for sub-surface marine layers. In regional marine applications, forcing impact configurations with separate delta-corrected factors can also break internal multi-variable physical consistency (Omstedt et al., 2012). By contrast, our application of the MLS method directly addresses these deficiencies. By adjusting absolute temperature fields while fully preserving dynamically simulated variance, daily non-linear trends, and vertical convective signatures generated by the HBM ensemble, our approach offers a far more robust framework for evaluating threshold-dependent risks under non-stationary climate conditions.

4.2 Applied implications of divergent regional warming trajectories

The multi-model projections completed under the high-emission RCP8.5 pathway reveal a significant and accelerated warming trend across both epicontinental domains, but their divergent climate trajectories dictate highly distinct regional adaptation priorities. The open North Sea maintains a relatively homogeneous thermal response, keeping seasonal shifts below 2 °C in the near-future and rising towards ∼3 °C by the end of the century. This slower, more buffered physical trajectory is driven by the basin's higher thermal capacity and vigorous exchange with the open Atlantic Ocean. From an operational and applied management perspective, this means climate risks in the open North Sea will manifest as steady baseline shifts. This chronic baseline warming will primarily impact demersal habitats — such as forcing the slow, continuous northward migration of cold-water commercial fish stocks like Atlantic cod — rather than triggering sudden, localised seasonal shocks.

Conversely, the semi-enclosed Baltic Sea undergoes severe, amplified seasonal shifts that demand immediate, highly localised risk-management strategies. This regional intensification is most prominent in the far northern and eastern catchments during late spring and early summer. The rapid warming projected for the Bothnian Bay ($> 5\,°C$) and the Gulf of Finland ($> 4\,°C$) represents a regional manifestation of Arctic amplification feedback mechanisms. In these shallow, brackish environments, the projected reduction in the extent and duration of winter ice cover alters the regional albedo, accelerating solar heat absorption during spring and summer.

This localised physical acceleration has immediate, high-impact consequences for regional environmental applications. In the Gulf of Finland and Bothnian Bay, the intense spring and summer warming will dramatically accelerate water column stratification, compounding seasonal hypoxia in deep basins and expanding macro-benthic dead zones (Polyakov et al., 2022). For coastal municipalities, this rapid thermal spike directly shifts the operational window for public health monitoring. The dramatic proliferation of warm-water days ($> 20\,°C$)—which historically were non-existent in these sub-arctic zones—will trigger earlier and more prolonged toxic cyanobacterial blooms and pathogenic *Vibrio* risks. Consequently, while the North Sea requires long-term structural adjustments for commercial fisheries, the northern and eastern Baltic Sea regions demand immediate operational alerting frameworks for public health and coastal tourism safety.

https://doi.org/10.5194/egusphere-2026-4212
Preprint. Discussion started: 28 August 2026

4.3 Socio-ecological impacts on tourism and fisheries

Translating complex physical datasets into targeted sector-specific indices helps bridge the gap between regional hydrodynamic modeling and practical climate adaptation planning. Our multi-index approach reveals that high-end greenhouse gas trajectories will drive substantial environmental shifts, with direct socio-economic impacts on maritime economies.

For coastal tourism, the projected increase in summer SST suggests an extension of the beach tourism season in Denmark, Germany, and Sweden. However, this positive economic outlook is countered by serious ecological risks. The rapid expansion of warm-water days creates favorable conditions for pathogenic outbreaks, which could lead to seasonal beach closures and disrupt local coastal economies.

For commercial fisheries, the projected change in spring SBT poses a direct challenge to traditional stocks in the southern and central North Sea. Atlantic cod depend on cold bottom waters for successful egg development and larval survival (Van Der Meeren and Ivannikov, 2006; González-Irusta and Wright, 2015; Kjesbu et al., 2023). Our index shows that by the end of the century, optimal spawning temperatures ($5 - 7\,^{\circ}$C) will disappear from the study region during March and April. As benthic temperatures approach and breach the maximum tolerable limit of $9.6\,^{\circ}$C, a northward shift of commercial fishing grounds appears inevitable, which will require adaptive management strategies from regional fishing fleets.

4.4 Methodological limitations and uncertainties in bias-corrected projections

While the MLS approach significantly optimises the usability of absolute temperature thresholds, its application introduces specific structural uncertainties that require cautious interpretation. First, the accuracy of the corrected 3D fields remains inherently linked to the spatial and temporal fidelity of the SST products. For the sea surface, the calibration relies entirely on satellite-derived SST reconstructions, which are prone to systemic regional errors in high-latitude, cloud-dense marginal basins. Biases, calibration drifts, or algorithmic smoothing within the underlying observational products (as extensively documented in CMEMS (2024)) directly propagate into the calculated monthly bias factors (B_m). Because these empirical errors are treated as absolute baseline truths by the scaling equations, any structural misrepresentation of shallow coastal upwelling zones or seasonal gradients in the satellite product will inevitably distort the calibrated future climate projections.

Second, severe limitations exist when applying this bias-corrected dataset to the ice-covered sectors, such as the northern Bothnian Bay and the Gulf of Finland. The thermodynamic sea-ice module integrated into the current version of the HBM is highly idealised, lacking advanced multi-category dynamical and complex snow-cover feedback configurations. Consequently, while the bias correction improves open-water summer metrics, it may artificially disconnect surface temperatures from the non-linear ice-albedo feedbacks simulated by the model. Users must therefore exercise caution when extracting variables from this dataset to force downstream indicator systems in seasonally ice-covered waters.

Finally, a fundamental theoretical weakness of linear scaling methodologies is their potential to violate internal physical conservation laws and disrupt multi-variable consistency. Adjusting temperature fields independently of co-dependent hydrodynamic variables (e.g., salinity, baroclinic velocity vectors, and vertical density stratification) can introduce localised thermodynamic imbalances into the three-dimensional water column. For instance, shifting the absolute benthic temperature without

https://doi.org/10.5194/egusphere-2026-4212
Preprint. Discussion started: 28 August 2026

a corresponding adjustment to the ambient salinity may artificially alter the calculated seawater density, thereby modifying local pressure gradients and geostrophic current shear. While this decoupling does not retroactively impact the decoupled ocean model's circulation fields, it implies that the bias-corrected absolute temperature fields must be interpreted primarily as independent, sector-specific biophysical indicators rather than a dynamically balanced, fully conservative thermodynamic system.

5 Conclusions

This study indicates that high-resolution regional hydrodynamic ensembles, when coupled with targeted bias correction, provide essential three-dimensional projections for regional climate adaptation planning. Validating historical simulations remains a critical step to identify and correct systematic seasonal errors that would otherwise distort threshold-dependent impact metrics. Under the high-emission RCP8.5 scenario, both the North and Baltic Seas are projected to experience significant warming by the end of the 21st century, with the landlocked Baltic basin acting as a primary warming hotspot. Converting these physical temperature fields into applied indicators clearly illustrates the potential socio-ecological consequences, including an extended but higher-risk summer tourism season and a projected northward shift in commercial cod spawning grounds. Future research should expand this multi-index framework to investigate additional hydrodynamic parameters, such as sea-level variations, salinity shifts, indicators relating to acidification and oxygen depletion, and circulation changes, to support comprehensive marine spatial planning and climate adaptation strategies.

Code and data availability. The HBM model source code, configuration files, and processed regional monthly mean datasets used to generate the figures and sector-specific indices are archived and maintained by the Danish Meteorological Institute (DMI) and the Federal Maritime and Hydrographic Agency (BSH). Data can be made available upon request to the corresponding author. Satellite SST Climate Data Records are accessible via the Copernicus Marine Environment Monitoring Service (CMEMS).

Author contributions. BME and JS designed the regional ocean climate experiments and developed the monthly linear scaling bias correction methodology. JS, KSM and BME executed the high-resolution nested HBM climate simulations. JS and KSM managed the EURO-CORDEX atmospheric forcing ensembles. BME performed the statistical validation and calculated the tourism and fishery indices. FJ provided project supervision and institutional coordination. BME prepared the manuscript draft, with critical reviews and edits contributed by all co-authors.

Competing interests. The authors declare that they have no conflict of interest.

https://doi.org/10.5194/egusphere-2026-4212
Preprint. Discussion started: 28 August 2026

Acknowledgements. The authors express their gratitude to the Climate Service Center Germany (GERICS) for coordinating and providing the EURO-CORDEX regional atmospheric climate forcing fields. We acknowledge the Deutscher Wetterdienst (DWD) for providing the high-performance computing resources necessary to run the multi-member HBM regional hydrodynamic simulations. Portions of this work were supported by institutional funding from the Federal Maritime and Hydrographic Agency (BSH) and the Danish Meteorological Institute (DMI). This work in DMI part is co-funded by the Danish Klimaatlas and the Danish National Centre for Climate Research (NCKF) projects. Danish Klimaatlas and NCKF are funded by the Danish State. At BSH this work was carried out as part of the DAS core service on behalf of the German Federal Ministry of Transport.

https://doi.org/10.5194/egusphere-2026-4212
Preprint. Discussion started: 28 August 2026

References

Andrée, E., Su, J., Larsen, M. A. D., Madsen, K. S., and Drews, M.: Simulating major storm surge events in a complex coastal region, Ocean Modelling, 162, 101802, https://doi.org/10.1016/j.ocemod.2021.101802, 2021.

Andrée, E., Drews, M., Su, J., Larsen, M. A. D., Dronen, N., and Madsen, K. S.: Simulating wind-driven extreme sea levels: Sensitivity to wind speed and direction, Weather and Climate Extremes, 36, 100422, https://doi.org/10.1016/j.wace.2022.100422, 2022.

Andrée, E., Su, J., Dahl Larsen, M. A., Drews, M., Stendel, M., and Skovgaard Madsen, K.: The role of preconditioning for extreme storm surges in the western Baltic Sea, Natural Hazards and Earth System Sciences, 23(5), 1817–1834, https://doi.org/10.5194/nhess-23-1817-2023, 2023.

Backhaus, J.: Climate-sensitivity of european marginal seas, derived from the interpretation of modelling studies, Journal of Marine Systems, 7(2), 361–382, https://doi.org/10.1016/0924-7963(95)00034-8, 1996.

Berg, P. and Poulsen, J. W.: Implementation details for HBM, Technical Report 12-11, Danish Meteorological Institute, Copenhagen, Denmark, 2012.

Carstensen, J. and Conley, D. J.: Baltic Sea Hypoxia Takes Many Shapes and Sizes, Limnology and Oceanography Bulletin, 28(4), 125–129, https://doi.org/10.1002/lob.10350, 2019.

Cheng, L., von Schuckmann, K., Abraham, J. P., Trenberth, K. E., Mann, M. E., Zanna, L., and Lin, X.: Past and future ocean warming, Nature Reviews Earth & Environment, 3(11), 776–794, https://doi.org/10.1038/s43017-022-00345-1, 2022.

Christensen, O. B., Kjellström, E., Dieterich, C., Gröger, M., and Meier, H. E. M.: Atmospheric regional climate projections for the baltic sea region until 2100, Earth System Dynamics, 13(1), 133–157, https://doi.org/10.5194/esd-13-133-2022, 2022.

E.U. Copernicus Marine Service Information (CMEMS): Quality Information Document (QUID) for Baltic Sea Sea Surface Temperature L4 & L3S Reprocessed Products (SST_BAL_SST_L4_REP_OBSERVATIONS_010_016 & SST_BAL_PHY_L3S_MY_010_040), Issue 3.0, https://documentation.marine.copernicus.eu/QUID/CMEMS-SST-QUID-010-016-040.pdf, technical report, 2024.

E.U. Copernicus Marine Service Information (CMEMS): Baltic Sea - High Resolution Reprocessed Sea Surface Temperature Analysis, Marine Data Store (MDS), Accessed on 01 Dec 2025, https://doi.org/10.48670/moi-00156, data set, 2026.

E.U. Copernicus Marine Service Information (CMEMS): Atlantic-European North West Shelf - Ocean In-Situ Near Real Time Observations, Marine Data Store (MDS), Accessed on 01 Dec 2025, https://doi.org/10.48670/moi-00045, data set, 2026.

Conley, D. J., Björck, S., Bonsdorff, E., Carstensen, J., Destouni, G., Gustafsson, B. G., and Zillén, L.: Hypoxia-Related Processes in the Baltic Sea, Environ. Sci. Technol., 43(10), 3412–3420, https://doi.org/10.1021/es802762a, 2009.

Conley, D. J., Carstensen, J., Aigars, J., Axe, P., Bonsdorff, E., Eremina, T., and Zillén, L.: Hypoxia Is Increasing in the Coastal Zone of the Baltic Sea, Environ. Sci. Technol., 45(16), 6777–6783, https://doi.org/10.1021/es201212r, 2011.

Cubasch, U., Waszkewitz, J., Hegerl, G., and Perlwitz, J.: Regional climate changes as simulated in time-slice experiments, Climatic Change, 31(2), 273–304, https://doi.org/10.1007/BF01095150, 1995.

Dangendorf, S., Frederikse, T., Chafik, L., Klinck, J. M., Ezer, T., and Hamlington, B. D.: Data-driven reconstruction reveals large-scale ocean circulation control on coastal sea level, Nature Climate Change, 11(6), 514–520, https://doi.org/10.1038/s41558-021-01046-1, 2021.

Dieterich, C., Wang, S., Schimanke, S., Gröger, M., Klein, B., Hordoir, R., and Meier, H. E. M.: Surface Heat Budget over the North Sea in Climate Change Simulations, Atmosphere, 10(5), 272, https://doi.org/10.3390/atmos10050272, 2019.

Diffenbaugh, N. S., Singh, D., Mankin, J. S., Horton, D. E., Swain, D. L., Touma, D., and Rajaratnam, B.: Quantifying the influence of global warming on unprecedented extreme climate events, Proceedings of the National Academy of Sciences, 114(19), 4881–4886, https://doi.org/10.1073/pnas.1618082114, 2017.

Ducrotoy, J.-P. and Elliott, M.: The science and management of the North Sea and the Baltic Sea: Natural history, present threats and future challenges, Marine Pollution Bulletin, 57(1), 8–21, https://doi.org/10.1016/j.marpolbul.2008.04.030, 2008.

Dulvy, N. K., Rogers, S. I., Jennings, S., Stelzenmüller, V., Dye, S. R., and Skjoldal, H. R.: Climate change and deepening of the North Sea fish assemblage: a biotic indicator of warming seas, Journal of Applied Ecology, 45(4), 1029–1039, https://doi.org/10.1111/j.1365-2664.2008.01488.x, 2008.

Engelhard, G. H., Righton, D. A., and Pinnegar, J. K.: Climate change and fishing: a century of shifting distribution in North Sea cod, Global Change Biology, 20(8), 2473–2483, https://doi.org/10.1111/gcb.12513, 2014.

Feser, F., Rockel, B., von Storch, H., Winterfeldt, J., and Zahn, M.: Regional Climate Models Add Value to Global Model Data: A Review and Selected Examples, Bulletin of the American Meteorological Society, 92(9), 1181–1192, https://doi.org/10.1175/2011BAMS3061.1, 2011.

Fu, W., She, J., and Dobrynin, M.: A 20-year reanalysis experiment in the Baltic Sea using three-dimensional variational (3DVAR) method, Ocean Science, 8(5), 827–844, https://doi.org/10.5194/os-8-827-2012, 2012.

Good, S. A., Martin, M. J., and Rayner, N. A.: EN4: Quality controlled ocean temperature and salinity profiles and objective analyses with uncertainty estimates, Journal of Geophysical Research: Oceans, 118(12), 6704–6716, https://doi.org/10.1002/2013JC009067, 2013.

González-Irusta, J. M. and Wright, P. J.: Spawning grounds of atlantic cod (*Gadus morhua*) in the north sea, ICES Journal of Marine Science, 73(2), 304–315, https://doi.org/10.1093/icesjms/fsv180, 2015.

Gordó-Vilaseca, C., Costello, M. J., Coll, M., Jüterbock, A., Reiss, H., and Stephenson, F.: Future trends of marine fish biomass distributions from the North Sea to the Barents Sea, Nature Communications, 15(1), 5637, https://doi.org/10.1038/s41467-024-49911-9, 2024.

Høyer, J. L. and Karagali, I.: Sea Surface Temperature Climate Data Record for the North Sea and Baltic Sea, Journal of Climate, 29(7), 2529–2541, https://doi.org/10.1175/JCLI-D-15-0663.1, 2016.

Huserbråten, M., Moland, E., and Albretsen, J.: Cod at drift in the North Sea, Progress in Oceanography, 167, 116–124, https://doi.org/10.1016/j.pocean.2018.07.005, 2018.

IPCC: Climate Change 2021: The Physical Science Basis. Contribution of Working Group I to the Sixth Assessment Report of the Intergovernmental Panel on Climate Change, Cambridge University Press, Cambridge, UK, https://doi.org/10.1017/9781009157896, 2021.

Jacob, D., Petersen, J., Eggert, B., Alias, A., Christensen, O. B., Bouwer, L. M., and Yiou, P.: EURO-CORDEX: New high-resolution climate change projections for European impact research, Regional Environmental Change, 14(2), 563–578, https://doi.org/10.1007/s10113-013-0499-2, 2014.

Jacob, D., Teichmann, C., Sobolowski, S., Katragkou, E., Anders, I., Belda, M., and Wulfmeyer, V.: Regional climate downscaling over Europe: perspectives from the EURO-CORDEX community, Regional Environmental Change, 20(2), 51, https://doi.org/10.1007/s10113-020-01606-9, 2020.

Kjesbu, O. S., Alix, M., Sandø, A. B., Strand, E., Wright, P. J., Johns, D. G., and Sundby, S.: Latitudinally distinct stocks of atlantic cod face fundamentally different biophysical challenges under on-going climate change, Fish and Fisheries, 24(2), 297–320, https://doi.org/10.1111/faf.12728, 2023.

Krupska, K. U., Speight, L., Robinson, J. S., Gilbert, A. J., and Cloke, H.: Forecasting bathing water quality in the UK: A critical review, WIREs Water, 11(4), e1718, https://doi.org/10.1002/wat2.1718, 2024.

https://doi.org/10.5194/egusphere-2026-4212
Preprint. Discussion started: 28 August 2026

Levitus, S., Antonov, J. I., Boyer, T. P., and Stephens, C.: Warming of the world ocean, Science, 287(5461), 2225–2229, https://doi.org/10.1126/science.287.5461.2225, 2000.

Madsen, K. S., Murawski, J., Blokhina, M., and Su, J.: Sea Level Change: Mapping Danish Municipality Needs for Climate Information, Frontiers in Earth Science, 7, 81, https://doi.org/10.3389/feart.2019.00081, 2019.

Meier, H. E. M., Broman, B., and Kjellström, E.: Simulated sea level in past and future climates of the Baltic Sea, Climate Research, 27(1), 59–75, https://doi.org/10.3354/cr027059, 2004.

Meier, H. E. M.: Baltic Sea climate in the late twenty-first century: a dynamical downscaling approach using two global models and two emission scenarios, Climate Dynamics, 27(1), 39–68, https://doi.org/10.1007/s00382-006-0124-x, 2006.

Meier, H. E. M., Andersson, H. C., Arheimer, B., Blenckner, T., Chubarenko, B., Donnelly, C., and Zorita, E.: Comparing reconstructed past variations and future projections of the Baltic Sea ecosystem—first results from multi-model ensemble simulations, Environmental Research Letters, 7(3), 034005, https://doi.org/10.1088/1748-9326/7/3/034005, 2012.

Meier, H. E. M., Väli, G., Naumann, M., Eilola, K., and Frauen, C.: Recently Accelerated Oxygen Consumption Rates Amplify Deoxygenation in the Baltic Sea, Journal of Geophysical Research: Oceans, 123(5), 3227–3240, https://doi.org/10.1029/2017JC013686, 2018.

Meier, H. E. M., Kniebusch, M., Dieterich, C., Gröger, M., Zorita, E., Elmgren, R., and Zhang, W.: Climate change in the Baltic Sea region: a summary, Earth System Dynamics, 13(1), 457–593, https://doi.org/10.5194/esd-13-457-2022, 2022.

Navarro-Racines, C., Tarapues, J., Thornton, P., Suklyankina, E., and Ramirez-Villegas, J.: High-resolution and bias-corrected CMIP5 projections for climate change impact assessments, Scientific Data, 7, 7, https://doi.org/10.1038/s41597-019-0343-8, data set, 2020.

Omstedt, A., Edman, M., Claremar, B., Frodin, P., Gustafsson, E., Humborg, C., Hägg, H., Mörth, M., Rutgersson, A., Schurgers, G., Smith, B., Wällstedt, T., and Yurova, A.: Future changes in the Baltic Sea acid–base (pH) and oxygen balances, Tellus B: Chemical and Physical Meteorology, 64, 19586, https://doi.org/10.3402/tellusb.v64i0.19586, 2012.

Pierce, D. W., Barnett, T. P., AchutaRao, K. M., Gleckler, P. J., Gregory, J. M., and Washington, W. M.: Anthropogenic Warming of the Oceans: Observations and Model Results, Journal of Climate, 19(10), 1873–1900, https://doi.org/10.1175/JCLI3723.1, 2006.

Pierce, D. W., Barnett, T. P., Santer, B. D., and Gleckler, P. J.: Selecting global climate models for regional climate change studies, Proceedings of the National Academy of Sciences, 106(21), 8441–8446, https://doi.org/10.1073/pnas.0900094106, 2009.

Polyakov, I. V., Tikka, K., Haapala, J., Alkire, M. B., Alenius, P., and Kuosa, H.: Depletion of Oxygen in the Bothnian Sea Since the Mid-1950s, Frontiers in Marine Science, 9, 917879, https://doi.org/10.3389/fmars.2022.917879, 2022.

Rahmstorf, S., and Coumou, D.: Increase of extreme events in a warming world, Proceedings of the National Academy of Sciences, 108(44), 17905–17909, https://doi.org/10.1073/pnas.1101766108, 2011.

Reckermann, M., Omstedt, A., Soomere, T., Aigars, J., Akhtar, N., Bełdowska, M., and Zorita, E.: Human impacts and their interactions in the baltic sea region, Earth System Dynamics, 13(1), 1–80, https://doi.org/10.5194/esd-13-1-2022, 2022.

Ridal, M., Olsson, E., Undén, P., Zimmermann, K., and Ohlsson, A.: HARMONIE regional reanalysis dataset for Europe, Uncertainties in Ensembles of Regional Re-Analyses (UERRA) Report, 2017.

Schroeder, K., Chiggiato, J., Josey, S. A., Borghini, M., Aracri, S., and Sparnocchia, S.: Rapid response to climate change in a marginal sea, Scientific Reports, 7(1), 4065, https://doi.org/10.1038/s41598-017-04455-5, 2017.

She, J. and Nielsen, J. W.: 'Silent' storm surge extremes in the western Baltic Sea on 4 January 2017, Journal of Operational Oceanography, 12, S111–S118, https://doi.org/10.1080/1755876X.2019.1633075, 2019.

Su, J.: HBM DKSS version 2013, Zenodo, https://doi.org/10.5281/zenodo.6769238, 2022.

Su, J., Murawski, J., Nielsen, J. W., and Madsen, K. S.: Regional wave model climate projections for coastal impact assessments under a high greenhouse gas emission scenario, Frontiers in Marine Science, 9, 910088, https://doi.org/10.3389/fmars.2022.910088, 2022.

Su, J., Murawski, J., Nielsen, J. W., and Madsen, K. S.: Coinciding storm surge and wave setup: A regional assessment of sea level rise impact, Ocean Engineering, 305, 117885, https://doi.org/10.1016/j.oceaneng.2024.117885, 2024.

Tian, T., Su, J., Boberg, F., Yang, S., and Schmith, T.: Estimating uncertainty caused by ocean heat transport to the North Sea: experiments downscaling EC-Earth, Climate Dynamics, 46(1), 99–110, https://doi.org/10.1007/s00382-015-2571-8, 2016.

Teutschbein, C. and Seibert, J.: Bias correction of regional climate model simulations for hydrological climate-change impact studies: Review and evaluation of different methods, Journal of Hydrology, 456-457, 12–29, https://doi.org/10.1016/j.jhydrol.2012.05.052, 2012.

Townhill, B. L., Couce, E., Tinker, J., Kay, S., and Pinnegar, J. K.: Climate change projections of commercial fish distribution and suitable habitat around north western Europe, Fish and Fisheries, 24(5), 848–862, https://doi.org/10.1111/faf.12773, 2023.

Tyrrell, T.: Anthropogenic modification of the oceans, Philosophical Transactions of the Royal Society A, 369(1938), 887–908, https://doi.org/10.1098/rsta.2010.0334, 2011.

Van Der Meeren, T. and Ivannikov, V. P.: Seasonal shift in spawning of atlantic cod (*Gadus morhua* L.) by photoperiod manipulation: egg quality in relation to temperature and intensive larval rearing, Aquaculture Research, 37(9), 898–913, https://doi.org/10.1111/j.1365-2109.2006.01510.x, 2006.

Wang, Y.-L. and Wu, C.-R.: Rapid Surface Warming of the Pacific Asian Marginal Seas Since the Late 1990s, Journal of Geophysical Research: Oceans, 127(12), e2022JC018744, https://doi.org/10.1029/2022JC018744, 2022.

https://doi.org/10.5194/egusphere-2026-4212
Preprint. Discussion started: 28 August 2026

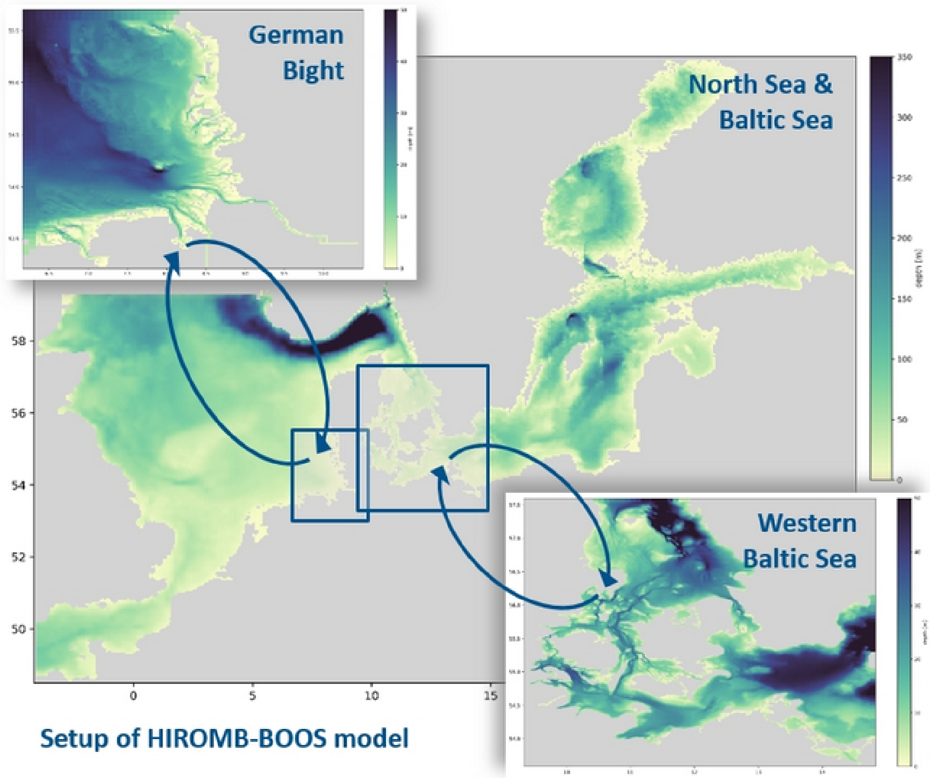

Figure 1. Setup and bathymetry of the HIROMB-BOOS Model (HBM) version 2.8 framework. Blue arrows present the dynamically interacting two-way nested grids between the parent domain (∼5.5 km) and sub-domains (∼1.8 km for German Bight; ∼0.9 km for Western Baltic Sea).

https://doi.org/10.5194/egusphere-2026-4212
Preprint. Discussion started: 28 August 2026

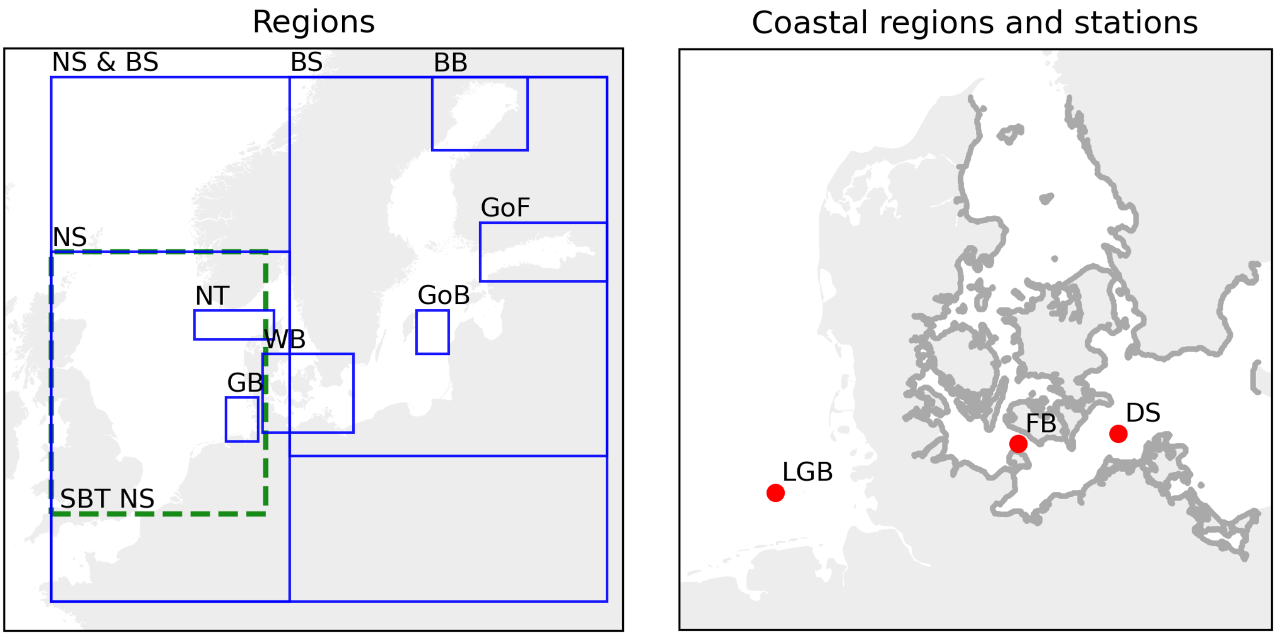

Figure 2. Geographic definitions outlining the regional polygons analyzed for sea surface temperature (SST) and sea bottom temperature (SBT) index (left map), alongside coastal areas highlighted for SST index and localized points tracking in-situ profiling validation arrays (right map). Regions label North Sea and Baltic Sea (NS & BS), Baltic Sea (BS), North Sea (NS), North Sea for sea bottom temperature (SBT NS), German Bight (GB), Norwegian Trench (NT), Western Baltic (WB), Gotland Basin (GoB), Bathnian Bay (BB), Gulf of Finland (GoF). Points label Lightship German Bight (LGB), Fehmarn Belt (FB), and Darss Sill (DS).

https://doi.org/10.5194/egusphere-2026-4212
Preprint. Discussion started: 28 August 2026

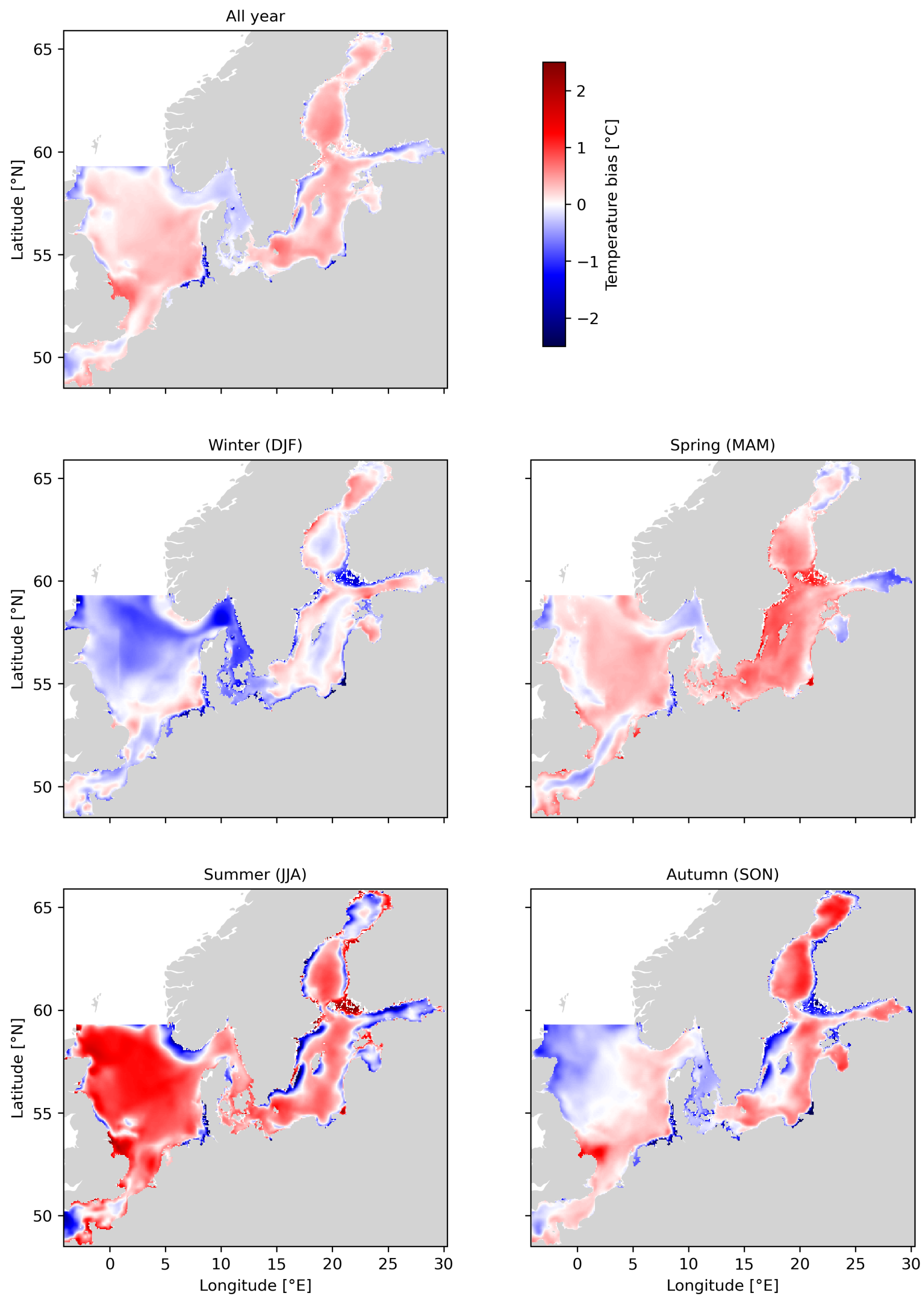

Figure 3. Spatial verification fields mapping annual and multi-seasonal sea surface temperature (SST) biases derived from the continuous reanalysis hindcast configuration relative to satellite Climate Data Records over the common timeframe 1982–2018. Positive values denote an overestimation of temperatures. Units are in °C.

https://doi.org/10.5194/egusphere-2026-4212
Preprint. Discussion started: 28 August 2026

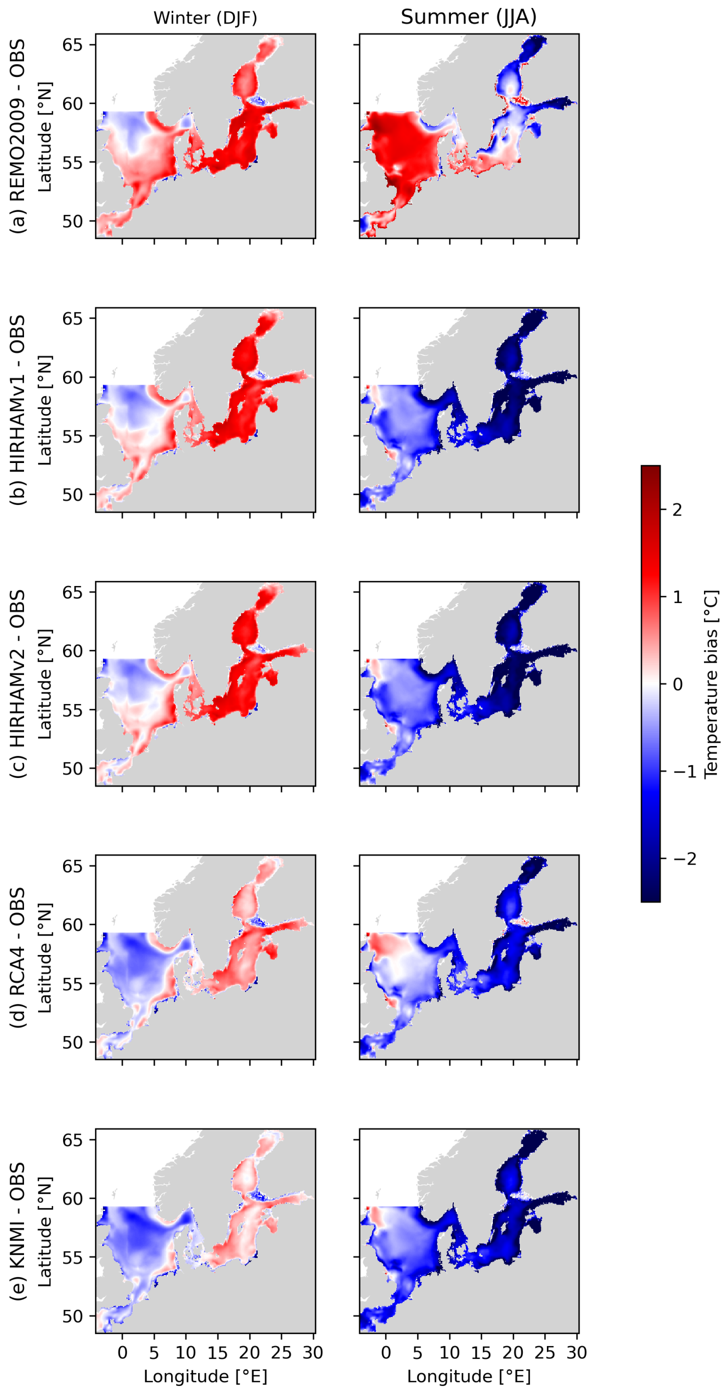

Figure 4. Multi-model discrepancy patterns tracking spatial sea surface temperature (SST) offsets across the five discrete climate forcing configurations relative to satcllite historical benchmarks during winter (DJF, upper panels) and summer (JJA, lower panels) horizons (1982–2005). Panels distinguish (a) REMO2009, (b) HIRHAMv1, (c) HIRHAMv2, (d) KNMI, and (e) RCA4 models. Units are in °C.

https://doi.org/10.5194/egusphere-2026-4212
Preprint. Discussion started: 28 August 2026

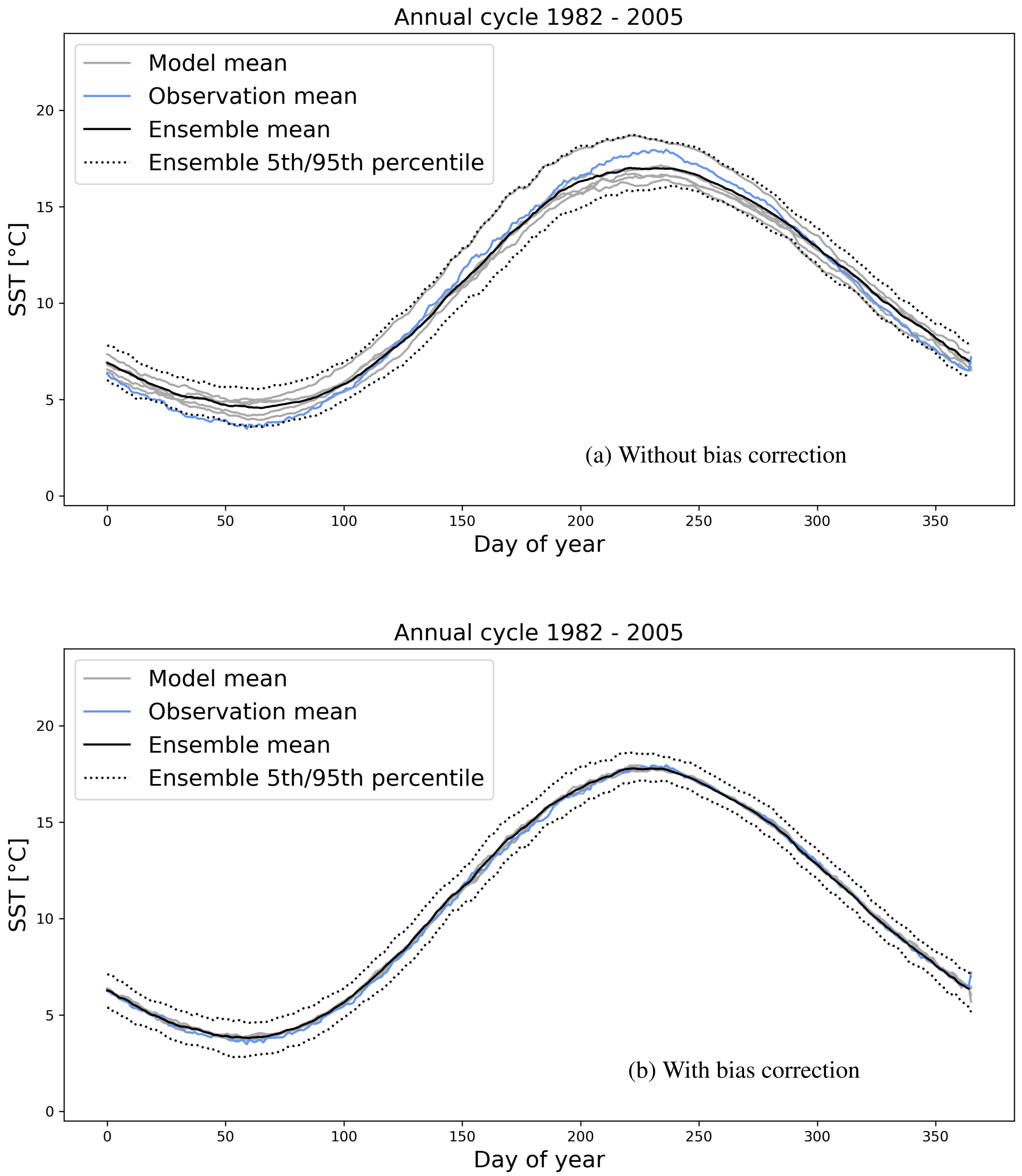

Figure 5. Climatological annual sea surface temperature (SST) progression envelopes computed at Station Lightship German Bight across the reference historical framework (1982–2005). Plots compare (a) uncorrected model envelopes alongside (b) corresponding Monthly Linear Scaling (MLS) calibrated curves evaluated relative to empirical satellite curves (blue curves).

https://doi.org/10.5194/egusphere-2026-4212
Preprint. Discussion started: 28 August 2026

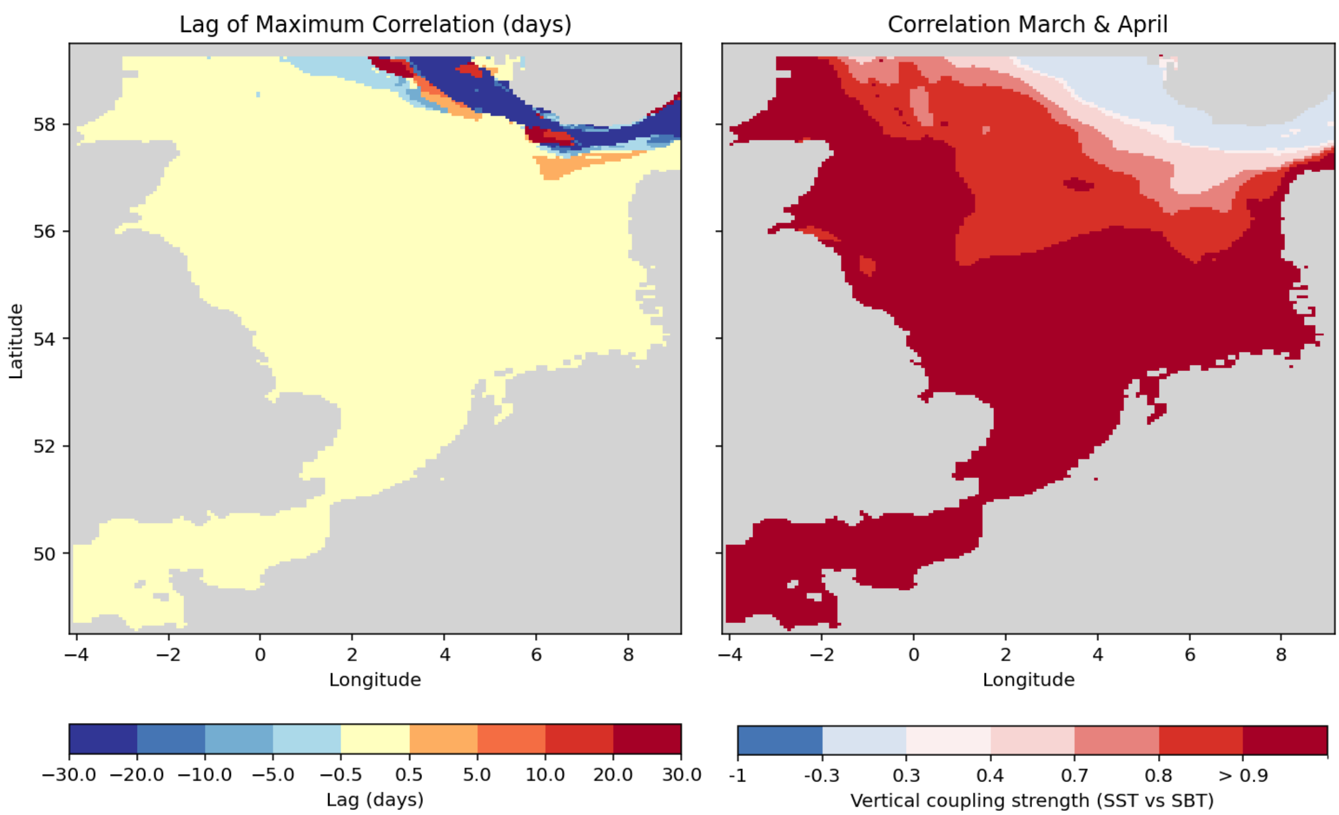

Figure 6. Spatial horizontal distribution presenting the temporal phase lag of maximum values (in days) (left) and the local vertical coupling strength (right) computed via cross-correlation between co-located sea surface temperature (SST) and sea bottom temperature (SBT) layers during the spring months March and April (1971–2000).

https://doi.org/10.5194/egusphere-2026-4212
Preprint. Discussion started: 28 August 2026

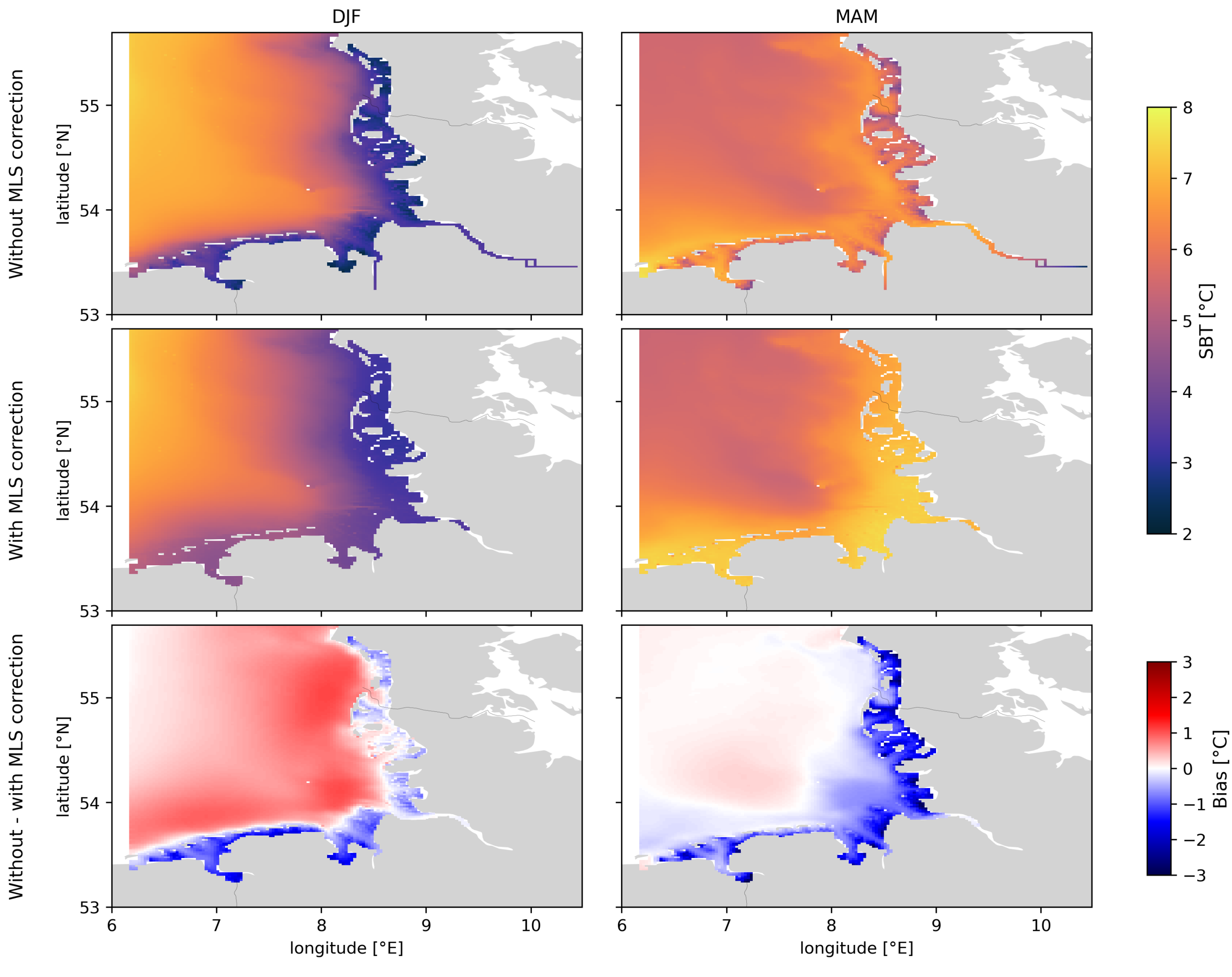

Figure 7. Spatial sea bottom temperature (SBT) distribution profiles simulated across the high-resolution German Bight coastal sub-domain for winter (DJF, left columns) and spring (MAM, right columns) seasons. Layers present raw values (top panels), MLS-calibrated values (middle panels), and the systematic absolute difference offset resolved between corrected and raw setups (bottom panels). Units are in °C.

https://doi.org/10.5194/egusphere-2026-4212
Preprint. Discussion started: 28 August 2026

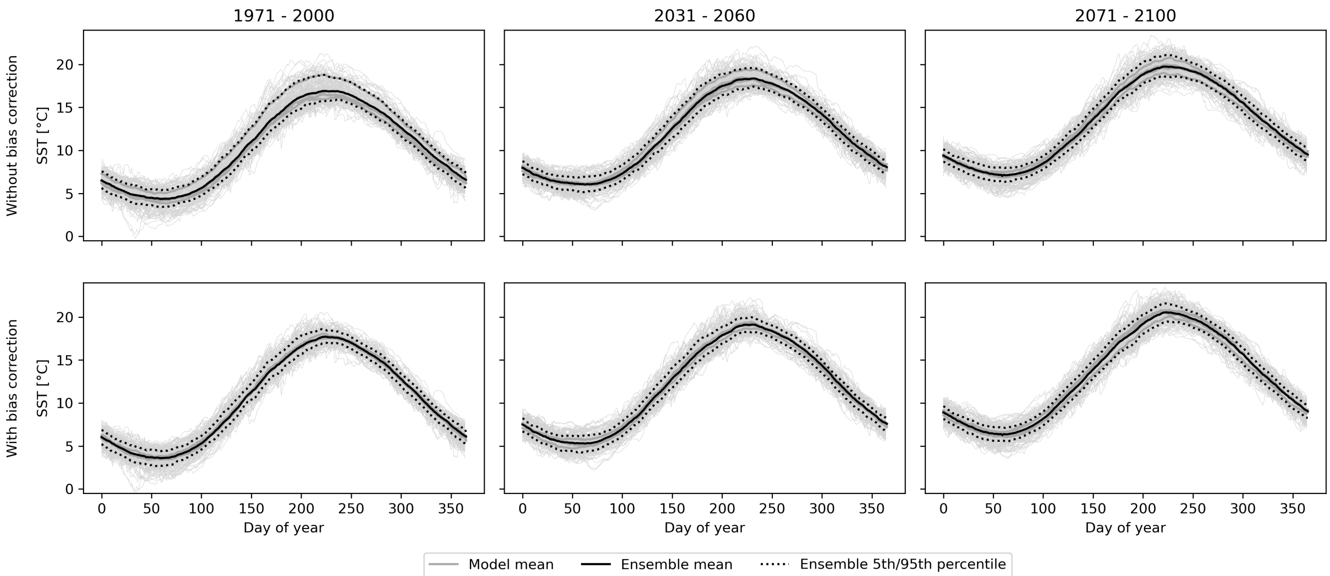

Figure 8. Multi-panel compilation showing daily resolved annual sea surface temperature (SST) curves simulated at station Lightship German Bight. Columns distinguish historical (left), near-future (middle), and far-future (right) projection slices. Rows separate raw, uncorrected output profiles (top) from monthly linear scaling (MLS) calibrated curves (bottom).

https://doi.org/10.5194/egusphere-2026-4212
Preprint. Discussion started: 28 August 2026

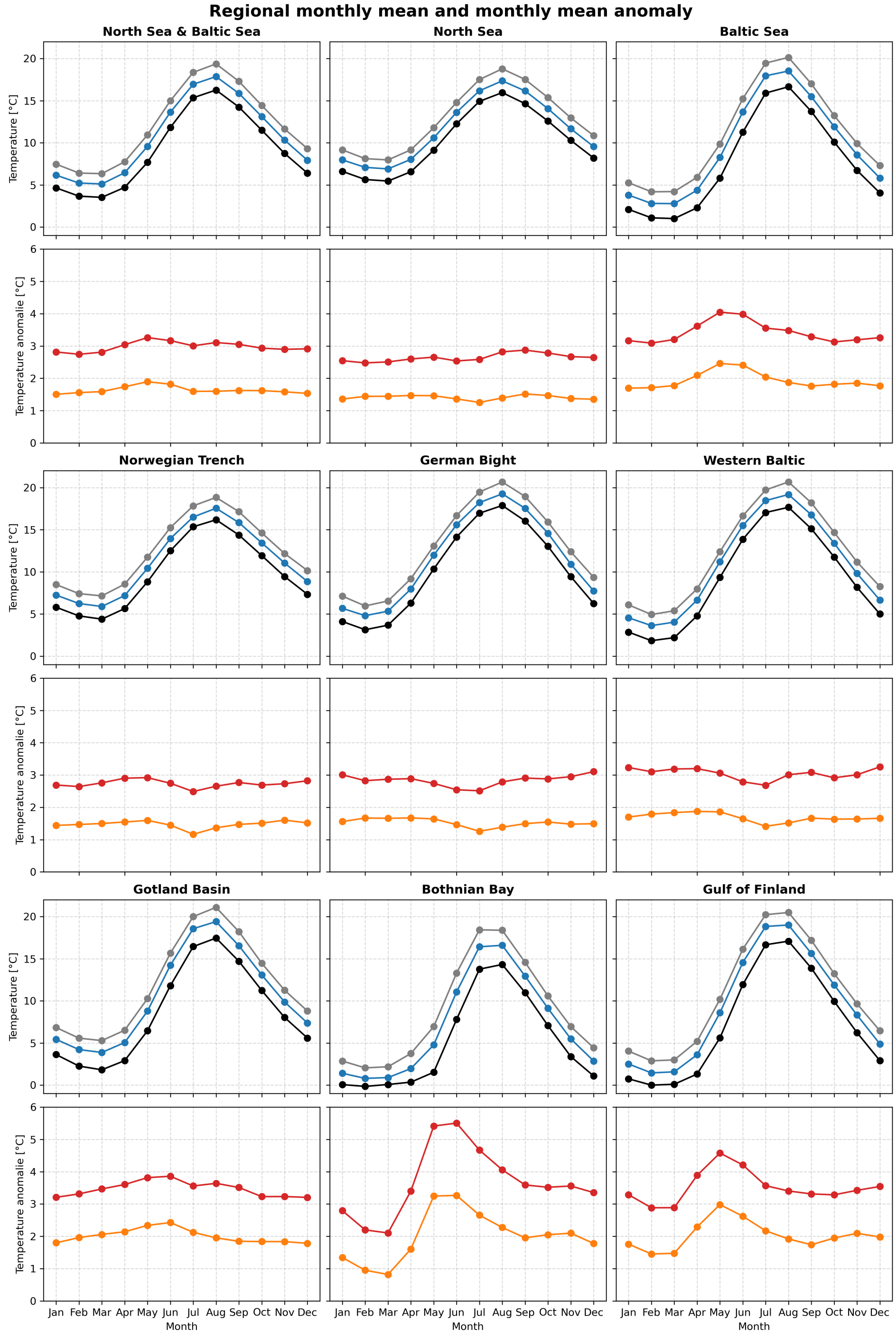

Figure 9. Compilation tracking regional multi-year monthly mean sea surface temperatures (top curves per panel) alongside matching anomaly curves (bottom curves per panel) across the comprehensive polygon zones outlined in Figure 2. Regional multi-year monthly mean sea surface temperatures are displayed for historical (black (1971–2000)), near-future (blue (2031–2060)) and far-future (grey (2071–2100)) periods. Anomalies sample shifts between historical timelines and near-future (orange curves) or far-future (red curves) envelopes.

https://doi.org/10.5194/egusphere-2026-4212
Preprint. Discussion started: 28 August 2026

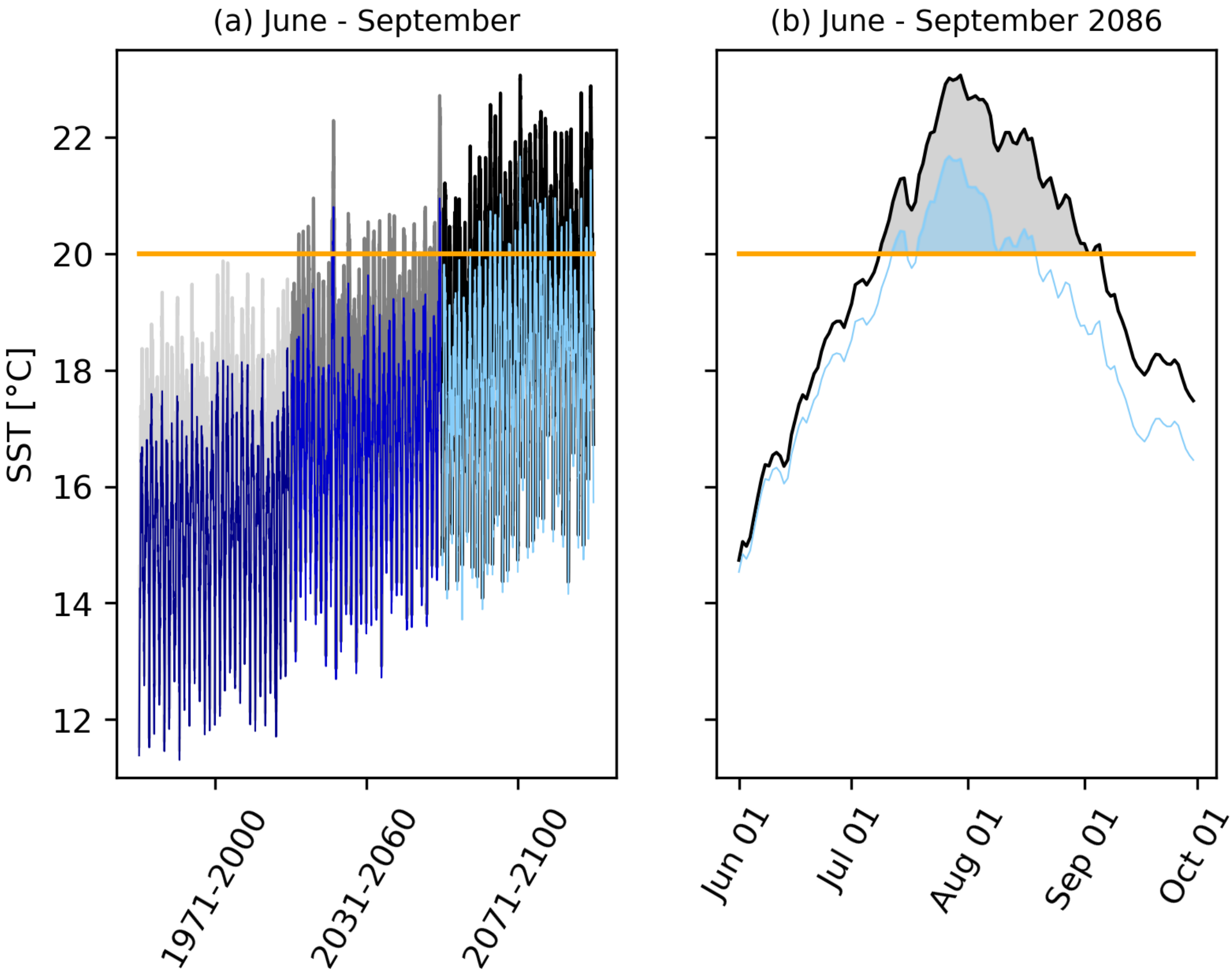

Figure 10. Bathing temperature index curves tracking surface thermal thresholds (> 20 °C, marked by the solid orange line) across shallow western Baltic coastal strips. Plot (a) shows the long-term historical-to-future projection trends. Plot (b) tracks daily resolved warming shifts during the simulation year 2086 to show differences between uncorrected (blue shades) and MLS-calibrated (grey/black shades) curves.

https://doi.org/10.5194/egusphere-2026-4212
Preprint. Discussion started: 28 August 2026

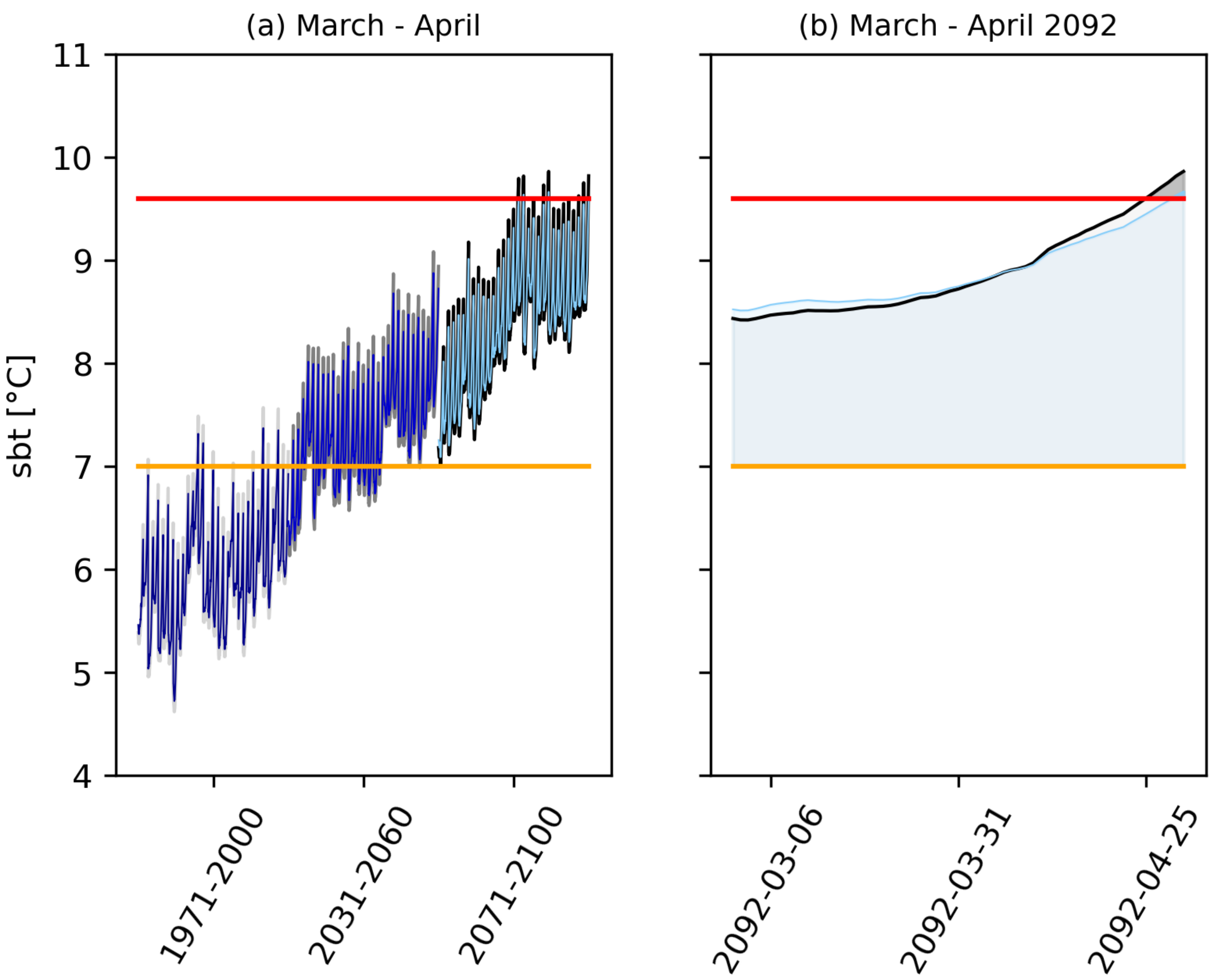

Figure 11. Fisheries spawning safety index curves tracking benthic spring water temperatures (March and April) in the North Sea polygon relative to two bio-thresholds: optimal preferred spawning (7 °C, orange line) and maximum tolerable threshold (9.6 °C, red line). Panel (a) presents long-term projections; panel (b) isolates daily resolved variations during the representative simulation year 2092.

https://doi.org/10.5194/egusphere-2026-4212
Preprint. Discussion started: 28 August 2026

Table 1. Atmospheric regional climate models from the EURO-CORDEX multi-model framework utilized as hydrodynamic boundary drivers for the ocean model simulations.

Model Identifier Code	Official EURO-CORDEX Archival String
REMO2009	EUR-11_MPI-CSC_MPI-M-MPI-ESM-LR_rcp85_REMO2009_v1
HIRHAMv1	EUR-11_ICHEC-EC-EARTH_rcp85_r3i1p1_DMI-HIRHAM5_v1
HIRHAMv2	EUR-11_ICHEC-EC-EARTH_rcp85_r3i1p1_DMI-HIRHAM5_v2
KNMI	EUR-11.KNMI.ICHEC-EC-EARTH.r12i1p1.RACMO22E.v1
RCA4	EUR-11.SMHI.EC-EARTH.r12i1p1.RCA4

https://doi.org/10.5194/egusphere-2026-4212
Preprint. Discussion started: 28 August 2026

Table 2. Absolute multi-year minimum winter temperatures and maximum summer temperatures calculated for the ensemble mean at station Lightship German Bight, contrasting raw configurations against monthly linear scaling (MLS) bias-corrected curves.

Climatological Slice	**Raw SST Output (°C)**		**MLS-Corrected SST (°C)**	
	Winter Minimum	**Summer Maximum**	**Winter Minimum**	**Summer Maximum**
Satellite data (1982–2000)	-0.3	21.1		
Historical (1971–2000)	2.4	18.1	1.7	18.9
Near Future (2031–2060)	4.2	20.5	3.5	21.3
Far Future (2071–2100)	5.4	21.0	4.7	21.8

https://doi.org/10.5194/egusphere-2026-4212
Preprint. Discussion started: 28 August 2026

Table 3. Projected regional variations in sea surface temperature anomalies (in °C) from the historical baseline period (1971–2000) to the near-future slice (2031–2060), broken down by annual mean and seasonal periods.

Target Geographical Region	Annual Mean	DJF	MAM	JJA	SON
North Sea & Baltic Sea	1.6	1.5	1.7	1.7	1.6
North Sea	1.4	1.4	1.5	1.3	1.5
Baltic Sea	1.9	1.7	2.1	2.1	1.8
Norwegian Trench	1.5	1.5	1.6	1.3	1.5
German Bight	1.5	1.6	1.7	1.4	1.5
Western Baltic	1.7	1.7	1.9	1.5	1.7
Gotland Basin	2.0	1.9	2.2	2.2	1.8
Bothnian Bay	2.0	1.4	1.9	2.7	2.0
Gulf of Finland	2.0	1.7	2.3	2.2	1.9

https://doi.org/10.5194/egusphere-2026-4212
Preprint. Discussion started: 28 August 2026

Table 4. Projected regional changes in sea surface temperature anomalies (in °C) from the historical reference baseline (1971–2000) to the far-future slice (2071–2100), broken down by annual mean and seasonal periods.

Target Geographical Region	Annual Mean	DJF	MAM	JJA	SON
North Sea & Baltic Sea	3.0	2.8	3.0	3.1	3.0
North Sea	2.6	2.6	2.6	2.7	2.8
Baltic Sea	3.4	3.2	3.6	3.7	3.2
Norwegian Trench	2.7	2.7	2.9	2.6	2.7
German Bight	2.8	3.0	2.8	2.6	2.9
Western Baltic	3.0	3.2	3.2	2.8	3.0
Gotland Basin	3.5	3.2	3.6	3.7	3.3
Bothnian Bay	3.7	2.8	3.6	4.7	3.6
Gulf of Finland	3.5	3.2	3.8	3.7	3.3

https://doi.org/10.5194/egusphere-2026-4212
Preprint. Discussion started: 28 August 2026

Table 5. Total cumulative number of days across each 30-year time slice when the spatially averaged sea surface temperature in western Baltic coastal waters breaches the 20 °C tourism and pathogens threshold, contrasting raw against bias-corrected configurations.

tophline **Climatological Core Period**	**Days Without Bias Correction**	**Days With Bias Correction**
Historical Baseline (1971–2000)	0	0
Near-Future Window (2031–2060)	41	318
Far-Future Window (2071–2100)	344	1329

https://doi.org/10.5194/egusphere-2026-4212
Preprint. Discussion started: 28 August 2026

Table 6. Total cumulative count of days during spring months (March and April) across 30-year slices when the spatially averaged sea bottom temperature in the North Sea polygon breaches the optimal cod spawning limit (7 °C) and maximum tolerable survival ceiling (9.6 °C).

Climatological Slice and Target Threshold	Days Without Bias Correction	Days With Bias Correction
Spring Preferred Boundary (7 °C)		
Historical Baseline (1971–2000)	45	78
Near-Future Horizon (2031–2060)	1366	1284
Far-Future Horizon (2071–2100)	1830	1830
Spring Survival Ceiling (9.6 °C)		
Historical Baseline (1971–2000)	0	0
Near-Future Horizon (2031–2060)	0	0
Far-Future Horizon (2071–2100)	6	35